High frequency ultrasonic studies of polyethylene

Keiichiro Adachi
Department of Polymer Science, Faculty of Science, Osaka University, Toyomaka, Osaka, Japan

and Gilroy Harrison and John Lamb
Department of Electronics and Electrical Engineering, Rankin Building, University of Glasgow, Glasgow, UK

and Alastair M. North and Richard A. Pethrick
Department of Pure and Applied Chemistry, Thomas Graham Building, University of Strathclyde, 295 Cathedral Street, Glasgow, UK
(Received 9 October 1980; revised 2 December 1980)

Ultrasonic measurements, covering the frequency range 5 MHz to 1 GHz, are reported on linear and branched polyethylene. At the lower frequencies the temperature dependence of the velocity and the amplitude of the absorption loss are consistent with observation of the familiar beta (β) and gamma (γ) relaxation processes. Studies as a function of the thermal history of the samples indicate that the detailed attenuation profile and the magnitude of the velocity are sensitive to crystallinity, reflecting changes in the branched chain content and lamella thickness. Data are also reported illustrating how the morphological changes of drawing and annealing influence the acoustic propagation parameters. The high frequency attenuation is due to the γ-macromolecular conformational relaxation, crystalline spherulite-amorphous region thermoelastic heat flow and spherulite-phonon scattering.

INTRODUCTION

Despite a number of acoustic investigations[1-12] of polyethylene during the past fifteen years, no complete correlation of the effects of morphology on both the acoustic absorption and velocity appears to exist. Most of the previous studies have been carried out at what is now considered to be the lower end of the available frequency range, and as such have been closely related in concept to high frequency dynamic mechanical testing. A preliminary study[1] of acoustic losses over the wider frequency range 5 MHz to 1 GHz indicated the existence of a variety of attenuation mechanisms sensitive to the detailed morphology of the polymer. Consequently, the investigation reported here was undertaken in an attempt to explore systematically the effects of change of morphology on both the ultrasonic attenuation and the velocity.

Polyethylene (PE) exhibits three distinct major relaxation processes[13]. The highest temperature process (α) is associated with molecular reorientational motion within the crystalline phase[14,15]. Mechanical studies on samples which have been subjected to an applied stress indicate the presence of a minor transition in this region which has been ascribed to reorientational motion of the crystalline domains themselves and is designated the α' process[16]. Two lower temperature relaxation processes have been observed using both mechanical and dielectric methods. The higher temperature process (β) appears to be associated with the micro-Brownian reorientational motion of the chains in the amorphous region[13], whereas the lower temperature (γ) process is ascribed to small scale motion[17-20] of polymer chains both in amorphous and crystalline regions[17,18]. The γ process has been found to be sensitive to chemical crosslinking, the amplitude of the loss decreasing with increasing crosslink density[19]. Each of these processes should be observable at appropriate temperatures and frequencies. Their identification and quantification should be assisted by extension of observations to higher frequencies, and by more careful consideration of other attenuation mechanisms. Furthermore, the inter-relationship with the morphology requires clarification.

EXPERIMENTAL

Characteristics of polymers

The samples of polyethylene were of commercial origin and their characteristics are summarized in *Table 1*. The molecular weights were determined by gel permeation chromatography. The densities of the samples were determined by a flotation method[21]. The melt temperatures, T_m, were determined using a Perkin-Elmer DSC-1 differential scanning calorimeter.

0032-3861/81/081032-08$02.00

Table 1 Characteristics of polyethylene samples

Code	Source	Trade name	Molecular weight M_w	Volume fraction of crystalline phase (%)	Density at 298K (kg m^{-3} x 10^{-3})	Melt temperature (K)	Lamella thickness (nm)
P1	B.P.	Rigidex	7500	81	970	409.6	55
P2	B.P.	Rigidex	13000	78	966	410.1	60
P3	B.P.	Rigidex	29000	75	962	409.3	52
P4	M.B.		30000	70	954	406.3	33
P5	M.B.		10000	76	963	408.7	47
P6	M.B.		10000	81	970	409.2	49
P7	B.V.			48	923	384.9	8
P8	S			47	922	385.1	8
P9	S			51	926	389.2	10

B.P. – British Petroleum
M.B. – Metal Box
B. V. – British Vistanex
S – Shell

Table 2 Chain branching characteristics

N.m.r. shifts (ppm)	39.6	38.2	37.7	34.7	34.3	32.9	32.2	27.4	23.4	22.8
assignment	n_2	$n_4 + n_5 + n_{6+}$	$2n_1$	$2n_4 + 3n_5 + 3n_{6+}$	$n_2 + n_4$	n_5	n_6	$2n_2 + 2n_4 + 2n_5$ n_4 $+ 3n_{6+}$		$n_5 + n_{6+}$

Sample		P_1	P_2	P_3	P_4	P_5	P_6	P_7	P_8
Branches per 1000 CH_2	C_1	0	0	0	3–4	0	0	0	0
	C_2	0	0	0	0	1	0	4	3
	C_3	0	0	0	0	0	0	0	0
	C_4	0	0	0	0	1	0	6	5
	C_5	0	0	0	0	0.3	0	2	2
	C_{6+}	–	0.2–0.6	0.2–0.5	0	1	0.5–1.3	2–4	2–4
Total		0.1–0.2	0.2–0.6	0.2–0.5	3–4	3	0.5–1.3	14–16	12–14

Estimation of chain branching in polymers

^{13}C n.m.r spectra permit quantitative estimation of the extent and nature of branching in normal alkane polymers[22]. The spectra used in this study were obtained by Dr F. Heatley of Manchester University, using a Varian SC 300 spectrometer. The polymers were dissolved in a mixture of *ortho*-dichlorobenzene and deuterobenzene, and the spectra recorded at approximately 400K using ^1H noise decoupling at a frequency of 75.5 MHz. Approximately 100000 transients were collected at an acquisition rate of 0.34 s^{-1}. The chemical shifts were recorded relative to TMS as internal standard. Under these conditions the spectra of the terminal methyl groups are saturated as a consequence of their long T_1 values. The peaks used in the analysis, *Table 2*, were assigned to CH_2 groups in specific structures[22]. Since these structures are chemically similar, their T_1 values are also assumed to be similar, allowing the composition of the polymer to be deduced by a direct comparison of the relative intensities. An estimate of the uncertainty of the analysis is included in *Table 2*.

Preparation of samples for ultrasonic study

The samples used in this study were of two types; thin films and slabs/rods. The thickness was governed by the frequency used in the acoustic attenuation experiments. Plots of attenuation *versus* thickness were used to determine the value of the attenuation coefficient at a particular frequency.

Films and thin discs were prepared by making a sandwich of the molten polymer between microscope slides, the thickness of the films being adjusted by use of selected spacers of known thickness. The polymer was fused in an oven at ~420K and then cooled. The plates were usually coated with a thin layer of silicone release agent prepared by dipping the glass slides in a dilute solution of silicon grease in hexane. The thicknesses were measured using a linear voltage differential transducer and were in the range 20 μm to 3 mm.

Slabs and rods of the polymer were prepared by melting the polymer at about 470K in a glass tube provided with a brass plunger and evacuated to a pressure of 10^{-2} torr. When the apparatus was opened slowly to atmospheric pressure the plunger was depressed to form a solid plug of polymer. The samples so prepared were then cooled to room temperature at a rate of about 0.05K s^{-1}. Discs of suitable thickness were finally machined on a lathe from the rods of diameter 30 mm.

The samples used in the annealing experiments were held in an oven for a specified period at a temperature defined with a precision of $\pm$1K. Where the period exceeded 3 h, the oven was evacuated to a pressure of 10^{-2} torr to avoid possible degradation due to atmospheric oxidation. Drawn[23] samples were prepared at 340K using a draw speed of 0.16 mm s^{-1}.

Ultrasonic measurements

Ultrasonic attenuation measurements were performed

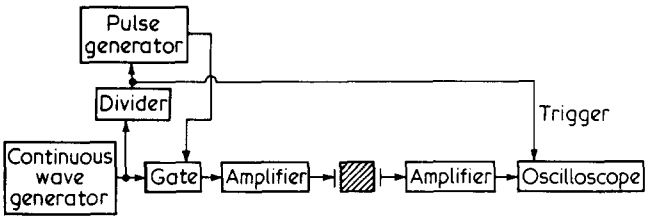

Figure 1 Schematic diagram of apparatus for velocity measurement

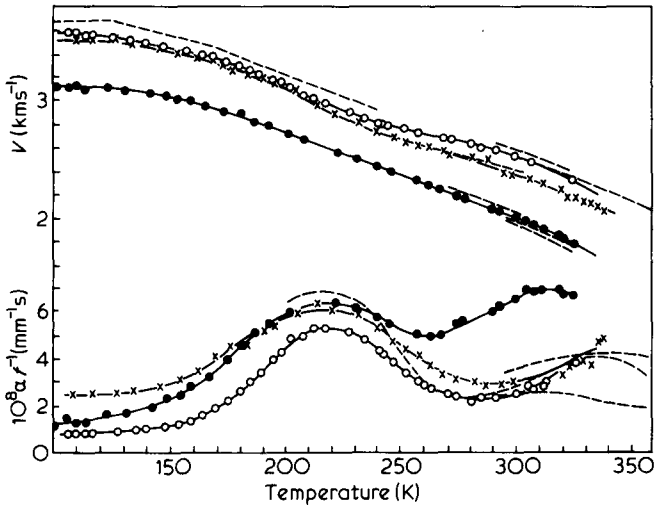

Figure 2 Temperature dependence of velocity v and attenuation divided by frequency, α/f, at 5 MHz. ○, P1; X, P4; ●, P8. Broken lines show the literature values for velocity and α/f data; high density refs. 3, 4, 5, 6, 8, 9 and low density refs. 5, 8, 11 polyethylene

in the frequency range 5 to 1000 MHz using an adaptation of the Watermann immersion method[24]. Details of the apparatus for studies in the frequency range 5 to 70 MHz[25] and 70 to 1000 MHz[1,26] have been described previously.

Ultrasonic velocity measurements were performed at 5 and 15 MHz using a method similar to that described by Arnold and Guenther[8]. The method is based on the accurate measurement of the time of flight of the pulse in the sample (*Figure 1*). A continuous wave is split into two parts, one part being divided by a factor of 2^n and the other applied directly to a switching circuit. The value of n is 12 for the measurements at 5 MHz. The output from the divider is a rectangular wave in phase with the original continuous wave and acts as a trigger for both a pulse generator and the oscilloscope. The pulse generator produces a rectangular pulse whose width, amplitude and delay are all completely variable yet locked to the original signal. By varying the delay time it is possible to observe both the excitation and various reflected pulses from the sample. The oscilloscope was equipped with a device to delay the start of the sweep thereby enabling a persistent picture to be obtained. The delay time was calibrated by observation of a continuous wave signal of variable frequency. With increasing delay time, the original pulse was observed followed by the detected signal. The delay was determined by measuring the separation in time between the tenth oscillation of each pulse. The velocity determined by this method is estimated to have a precision of better than ± 0.4 km s^{-1} at 15 MHz.

RESULTS AND DISCUSSION

Temperature dependence of sound attenuation and velocity

The temperature dependence of the attenuation and velocity at 5 MHz were investigated on high (P1), intermediate (P4) and low (P8) density samples of PE and the results are presented in *Figure 2*. Data from other authors[2-12] are also shown for comparison. For the low density P8 two relaxation regions were clearly delineated. It is useful to consider the position of the loss peaks on the temperature axis relative to other measurements on the dynamic properties[13,14,18,27-31] (*Figure 3*). Clearly the loss peaks in this sample coincide well with the β and γ processes. The variation in the amplitude of the β process (believed to be a glass–rubber transition) with polymer type is consistent with the known variations in amorphous content.

The temperature dependence of the velocity (dv/dt) changes in the region of the loss peaks (*Figure 2*).

The variation of the sound velocity with the decreasing modulus associated with thermal expansion has been reported by Schuyer[11] and by Wada and Yamamoto[32]. According to Schuyer, the temperature dependence of the longitudinal sound velocity v is given by

$$\frac{1}{v}\left[\frac{dv}{dT}\right] = \frac{A}{\rho}\left[\frac{\delta\rho}{\delta T}\right]_\sigma - \frac{1}{1-\sigma^2}\left[\frac{\delta\sigma}{\delta T}\right]_\rho \qquad (1)$$

where A, ρ and σ denote a constant, the density and the Poisson ratio, respectively. If we assume a Lennard–Jones intermolecular potential, implying purely van der Waals interactions between chains, the value of A is 3.17. The temperature dependence of velocity outside the relaxation regions (*Figure 2*) is consistent with the predictions of this equation.

The change in velocity due to an ideal single relaxation time process is

$$(v_\infty^2 - v_0^2)/v_\infty^2 = 2\alpha\lambda(\max)/\pi \qquad (2)$$

where α, v_∞ and v_0 denote respectively the attenuation per wavelength, and the velocity at high and low frequencies[33]. The term α (max) indicates the value of the acoustic loss for the condition $\alpha\lambda = 1$. The appropriate value of α being defined with reference to the correlation diagram (*Figure 3*). The relaxations are in practice somewhat broader than ideal and hence allowance has to be made for an effective underestimate of the increment based on

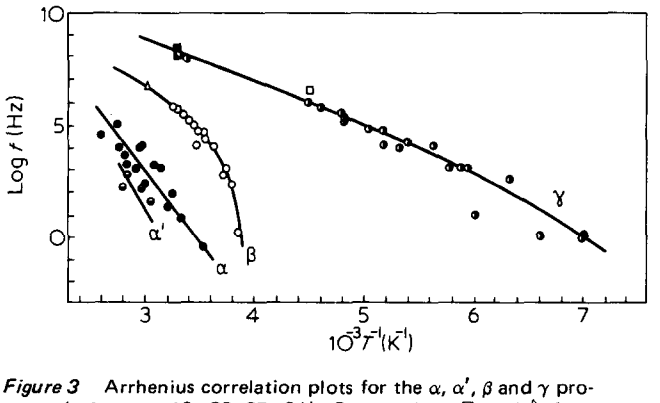

Figure 3 Arrhenius correlation plots for the α, α', β and γ processes (references 13–20, 27–31). Present data: □, and △, from temperature dependence of α/f. ■, and □, from frequency dependence of α/f

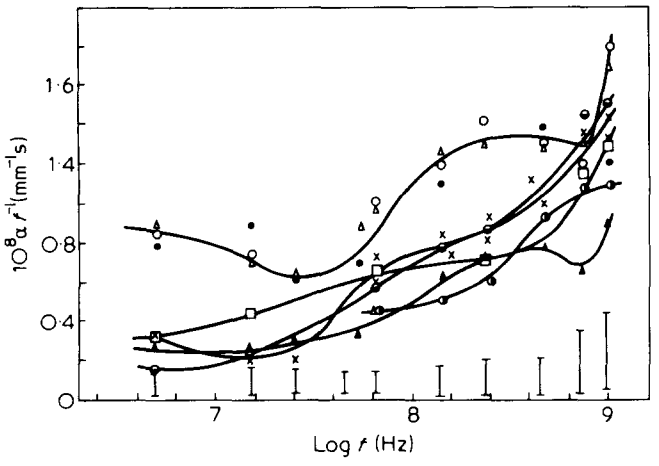

Figure 4 Frequency dependence of α/f for P1 and P7 at 298K. ○, P7 as received film; ●, P7 annealed at 378K for 46.5 h; △, P7 slowly cooled from melt with the rate 0.06K min^{-1}; X, P1 quenched; ◒, P1 slow cooling 4.4K min^{-1}; □, P1 slow cooling 2.0K min^{-1}; ▲, P1 slow cooling 0.06K min^{-1}; ◑, quenched and then annealed at 403K for 2 days

equation (2), this being performed on a semi-empirical basis. For polymer P8 this equation predicts a velocity change of 0.6 km s^{-1} through the β-process, similar to that found experimentally. However, low frequency observations of the γ-process show that it exhibits marked non-ideal (distributed relaxation time) behaviour, under which circumstance equation 2 grossly underestimates the velocity change. Semi-empirical allowance for this raises the 0.17 km s^{-1} predicted by equation 2 to 0.3 to 0.8 km s^{-1}, to be compared with the observed value of 0.9 km s^{-1}.

Thus the temperature dependence of velocity and attenuation at these lower frequencies can be ascribed to a superposition of thermal expansion and well recognised relaxation features.

Frequency dependence of attenuation

The frequency dependence of the attenuation of 298K is much more difficult to interpret (*Figure 3*). These curves are sensitive to the thermal history of the samples, but do show a maximum in the range 10^8–10^9 Hz and a steep rise around 10^9 Hz.

Inspection of the frequency–temperature correlation plot (*Figure 4*) allows the maximum to be assigned to the γ process, and by the same token the negative slopes at 5 MHz represent the high frequency tail of the β-process. It is noticeable that the γ-process is less sensitive to the amorphous/crystalline content than the glass-transition reflected in the β-process.

The attenuation at the highest frequencies is dependent on the sample morphology, and can be discussed in terms of thermoelastic and phonon scattering processes.

Thermoelastic absorption processes

The adiabatic passage of a sound wave is associated with a fluctuation in the local temperature of the transmitting medium. When viscothermal processes lead to heat transport between the peaks and troughs of this fluctuation, there arises classical viscothermal absorption familar in all homogeneous media. However, in heterogeneous media the wave may couple differently to different domains, and the temperature difference between domains may also lead to thermoelastic losses. In order to explain the total observed attenuation we consider calculated values for these processes.

The attenuation due to classical viscothermal absorption is calculated from the Stokes–Navier equation and is given by[34,35]

$$\alpha_T = \frac{2\pi^2 f^2}{\rho v^3}\left[\frac{\Lambda'}{C_v}\left(\frac{M_\sigma - M_\theta}{M_\theta}\right)\right] \quad (3)$$

where α_T, f, ρ, v, Λ', C_v, are, respectively, the attenuation, frequency, density, velocity, thermal conductivity and heat capacity at constant volume. M_σ and M_θ are, respectively, the adiabatic and isothermal moduli. For a longitudinal wave, the adiabatic modulus is given by

$$M_\sigma = K + (\tfrac{4}{3})G \quad (4)$$

where K and G are, respectively, the bulk and shear moduli. If we set[36,37] G_σ equal to $G_\theta = 1.1 \times 10^9$ N m^{-2}, $K = 4.8$ N m^{-2} $\rho = 9.60 \times 10^5$ kg m^{-3}, the thermal expansivity $a = 7.4 \times 10^{-4}$ K^{-1}, $v = 2.6 \times 10^3$ ms^{-1}, Cp to 2.05 J K^{-1} and Λ' to 0.5 J m^{-1} s^{-1} K^{-1} it is possible to evaluate α_T as a function of frequency. The results are illustrated in *Figure 5*, curve 5, where it can be seen that this process contributes only a minor fraction of the observed attenuation.

The other process to be considered is attenuation due to the finite time for intergranular conduction[38,39]. The

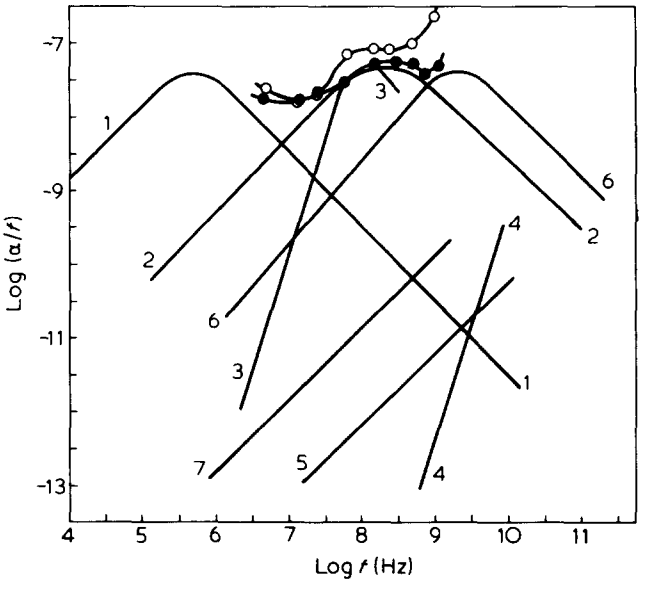

Figure 5 Comparison of the calculated and observed frequency dependence of α/f. ○, P1 quenched; ●, P1 slowly cooled (0.06K min^{-1}); curve 1, molecular relaxation for the β process; curve 2, molecular relaxation for the γ process; curves 1 and 2 are plotted so that the maximum value of α/f is equal to the observed maximum of α/f in the temperature dependence curve shown in *Figure 2*. The curves 1 and 2 were calculated assuming that the β and γ processes may be approximated to a single relaxation time and the appropriate values of f_0 were obtained from interpolation of the data in *Figure 4*. Curve 3, scattering due to spherulites calculated in terms of equation (9) with the value of a equal to 10 μm: curve 4, scattering due to lamellae, equation (9) $a \approx 10$ nm; curve 5, thermoelastic attenuation from equation (3); curve 6, inter-grain heat flow, equations (5), (6) and (7); curve 7, phonon–phonon interaction, equation (10)

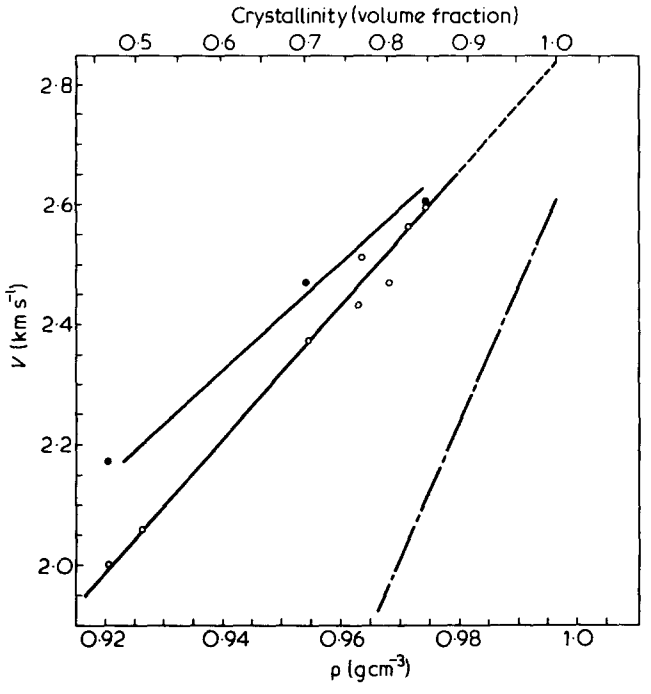

Figure 6 Correlation of the velocity with density ○, 4.96 MHz; ●, 15.3 MHz. Broken line, data by Davidse *et al.* at ~5 MHz

amplitude of the loss can be described[36] by

$$\alpha_{IF}=\frac{\pi}{v}\frac{C_p-C_v}{C_v}R\frac{f_0 f}{f_0^2+f^2} \tag{5}$$

where f_0 denotes a relaxation frequency, given for large domains by

$$f_0 \simeq \Lambda' \rho C_p L_c^2 \tag{6}$$

and the parameter R is given by

$$R=\frac{\langle (M-\langle M\rangle_{av})^2\rangle_{av}}{\langle M^2\rangle_{av}} \tag{7}$$

In the above equations L_c and M are the size and longitudinal modulus of the heterogeneous domains in the sample. The suffix *av* denotes the statistical average. PE consists of crystalline spherulites dispersed through an amorphous phase[40-42]. The size of the spherulites varies from 5 to 50 μm whereas the width of the crystalline lamellae or amorphous zones lie in the range 5 to 50 nm depending on the crystallinity of the material. To consider heat flow from one crystalline spherulite to another we substitute these dimensions in equation 6. This indicates that f_0 has a value of 10 kHz for 5 μm domains and would be less than 10 kHz for large domains. It is therefore reasonable to assume that the losses due to inter-spherulite heat flow can be ruled out because the characteristic frequency is much too low. A possibility is heat flow between crystalline lamellae and the amorphous zones. In order to estimate the modulus of the amorphous phase it is necessary to assume that the molecules behave similarly to those in the melt. Extrapolation of the temperature dependence of M for molten polyethylene at 12 MHz to the temperature of observation indicates that an appropriate value would be 2.3×10^9 N m^{-2} [9]. Extrapolation of a plot of velocity *versus* percentage crystallinity (*Figure 6*) indicates a value of 8.0 $\times 10^{-9}$Nm^{-2} for the crystalline phase. The velocity measured in this study is equivalent to the isotropic value obtained by extrapolation of the velocity data to the 100% value; it is of interest to note that this value lies between the anisotropic values which are respectively 320 G Mn^{-2} along the chain direction and 1–3 G Mn^{-2} perpendicular. These figures yield

$$R=0.41-0.35\chi \tag{8}$$

where χ is the volume fraction of the crystalline phase. For the quenched high density polymer (P1) the value of χ is 0.7 and the value of α/f calculated was found to be 4.5 $\times 10^{-8}$ s mm^{-1} at the frequency f_0. This value and the associated frequency dependence of (α/f) are comparable with those observed experimentally (*Figure 5* curve 6).

Thus the increase in α/f observed at the highest frequencies can be ascribed to a relaxation process involving heat flow between the crystallite lamellae and the contiguous amorphous zones.

Phonon scattering processes

Attenuation of the sound wave may occur as a consequence of scattering by inhomogeneities or defects and phonon–phonon interactions. Looking first at scattering by phase inhomogeneities, if the wavelength of the sound is larger than the size of the domain and multiple scattering is neglected, then the Rayleigh equation can be applied. Okano[43] has calculated the ultrasonic attenuation in the case of viscoelastic spheres suspended in a viscoelastic medium and obtained

$$\alpha_s=\frac{8\pi^4 f^4 a^3}{v^4}\left[\frac{1}{3}\left(\frac{K_1-K_0}{K_1}\right)^2+\left(\frac{\rho^1-\rho^0}{2\rho_1+\rho_0}\right)^2\right]\varphi \tag{9}$$

where a, K, ρ and φ denote the radius, bulk modulus, density and volume fraction, respectively. The suffixes 1 and 0 denote the spheres and continuous medium respectively. The value of α/f has a maximum around the frequency at which the wavelength is comparable with the size of the domain, although the attenuation in this condition is not described by the above equation. Several examples of the appropriate calculations have been described by Truell *et al*[44].

In order to assess whether appreciable scattering may be caused by either the individual lamellae or the spherulitic aggregates of lamellae appropriate values are substituted into equation 9. For the lamellae this calculation yields, for quenched high density P1, a value of 6×10^{-12} s mm^{-1}, which is much smaller than that observed experimentally.

For spherulites it is necessary to include the anisotropic response within the spherulitic structure. This anisotropy has been measured by Rider and Williamson[2], and for the purposes of this semi-quantitative calculation we use a mean modulus of 6.5 GPa. Use of equation 9 than predicts an attenuation at 50 MHz of 2.6×10^{-9} s mm^{-1} which (increasing with frequency) is comparable with the experimentally observed values.

It should be noted that in this case the wavelength is approximately 50 μm at 50 MHz, comparable with the spherulite domain size. Furthermore, above 250 MHz the thickness of the samples for the ultrasonic measurements was less than 70 μm. Consequently, the assumptions in the theory become less tenable at the higher frequencies, and

Table 3 Spherulites in sample P1

Cooling rate K min^{-1}	Diameter of spherulite μm	Position of increase in the frequency dependence of α/f MHz
~50	13 ± 3	100
4.4	13 ± 3	120
2.0	30 ± 5	50
0.06	35 ±	200

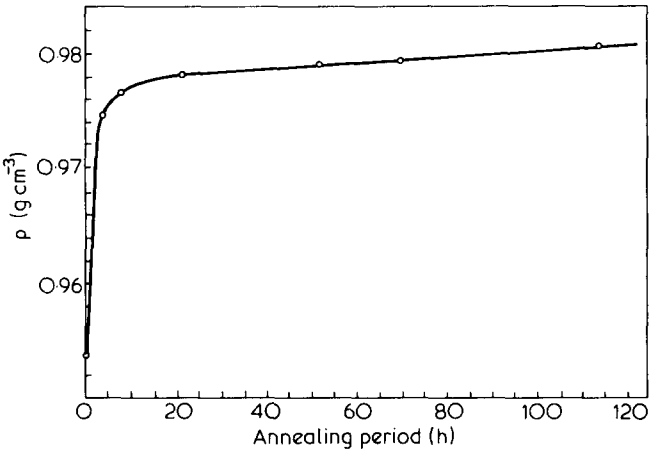

Figure 7 Effect of annealing at 403K on the density of the sample P1 measured at 298 K

this result can be considered as only semi-quantitative.

The sizes of the spherulites measured using polarizing microscopy are listed in *Table 3*. There is no precise correlation between the size of the spherulites and the wavelength at which absorption increases are observed. This is not surprising since the theory used contains a number of assumptions and approximations. Nevertheless, the general correspondence between prediction and theory leads to the proposition that such scattering is a significant cause of ultrasound attenuation.

It is rather unlikely that dislocation damping, well documented in metals[34,44], will occur in the same way in polymers. However, defect migration may very well be associated with molecular relaxation processes such as the γ-relaxation. Chain ends and branches, as well as 'kinks' in the chain contour all form 'defects' in both the crystalline and amorphous phases[45]. In addition, various types of dislocation exist[46,47]. All of these could facilitate relaxation by the 'defect diffusion' mechanism[48].

The existence of phonon–phonon scattering interactions may be predicted on the basis of the theory of Woodruff and Ehrenreich for both long- and short-lived phonons[49]. The lifetime of the phonon in PE at room temperature is of the order of 10^{-13} s and so is much shorter than the period of ultrasonic wave. We can predict the amplitude of the attenuation

$$\alpha_{pp} = \frac{4\pi^2 \gamma^2 f^2 \Lambda' T}{v^5} \qquad (10)$$

where γ denotes the Gruneisen constant. The other symbols have their usual meanings. With the aid of data on thermal conductivity and the published value of γ[50], we can calculate α_{p-p}, having a value of 1.3 mm^{-1} and 0.013 mm^{-1} at 1000 and 100 MHz respectively. These values are considerably smaller than the observed attenuation (*Figure 5* curve 7).

Thus the dominant attenuation processes are the molecular conformational relaxations (β and γ processes), crystallite–amorphous thermoelastic heat flow and phonon scattering by spherulites.

Annealing

Annealing effects are most pronounced in the samples of high crystallinity. For films of P1 annealed under vacuum at 403K the density and the acoustic attenuation both changed with time (*Figures 7* and *8*). The relationship between attenuation and density for measurements at 240 and 730 MHz is shown in *Figure 9*.

Investigations of the effect of annealing of polyethylene near its melting point have indicated the occurrence of lamella thickening[41,42,51]. However, the spherulite size does not necessarily alter. The frequency dependence of the difference in α/f between quenched and annealed samples (*Figure 10*) indicates a maximum at approximately 200 MHz and a further increase at appro-

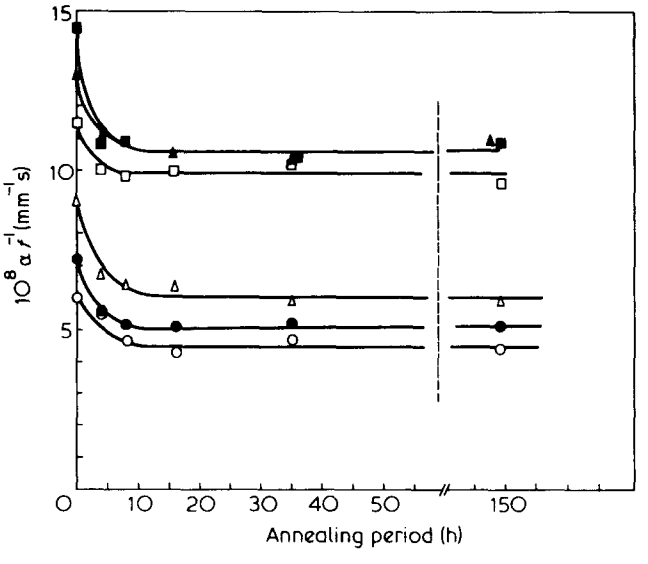

Figure 8 Effect of annealing on the value of α/f for the sample P1 at 298K. ○, 70 MHz; ●, 140 MHz; △, 240 MHz; □, 460 MHz; ▲, 730 MHz; ■, 1010 MHz

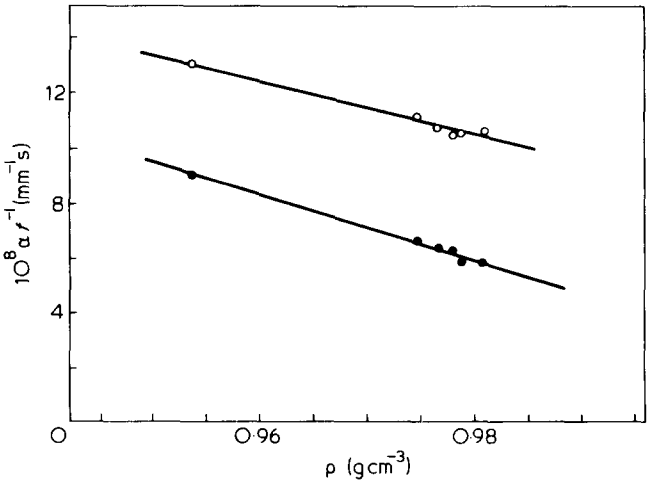

Figure 9 Correlation between the value of α/f and density for the annealed sample of P1. ○, 730 MHz; ●, 240 MHz

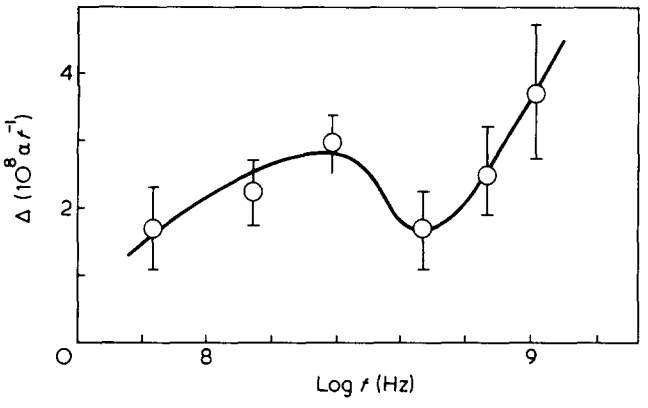

Figure 10 Frequency dependence of the difference in α/f between quenched and annealed samples of P1

ximately 1 GHz. The process at 200 MHz may be correlated with the γ process (see curve 2 of *Figure 5*) whereas the loss at 1 GHz appears to be associated with intergranular heat transfer. The observed changes on thermal treatment are consistent with changes in the lamella thickness, the intergranular heat loss moving its relaxation frequency to approximately 10 GHz and also decreasing in amplitude as represented by equation (8) together with equation (5).

To estimate the changes in the morphology more quantitatively we employ the relationship[52]

$$T_m = T_m^0(1 - 2\sigma_c/1_c\Delta h) \tag{10}$$

where T_m^0, σ_c and Δh denote the equilibrium temperature, the surface energy of the crystalline lamella and the heat of fusion per unit volume of the polymer respectively. For PE the values of these parameters are: $T_m^0 = 414.6$K, $\sigma_e = 90 \times 10^{-2}$J m^{-2} and $\Delta h = 2.18 \times 10^{10}$J m^{-3} [38]. If one assumes a clean-cut two phase model for the morphology, the thickness of the amorphous layer 1_a is given by

$$1_a = 1_c(1 - \chi)/\chi \tag{11}$$

where χ is the volume fraction of the crystalline phase. From the data on the melting points 1_a and 1_c were calculated with the aid of equations 10 and 11. The results are presented in *Figure 11*, and illustrate large changes in these dimensions.

The effect of annealing on the velocity was also examined. The measured velocity depended on the overall macroscopic density, and hence on the crystallinity in a way already introduced in *Figure 6* and discussed in more detail below.

Density, crystallinity, velocity relationship

An earlier study of the velocity of sound in a variety of PE samples indicated an approximate correlation of the density with the propagation velocity[10,11]. A similar study examining the polymers listed in *Table 1* at 5 and 15 MHz is presented here (*Figure 6*). The observations are similar to those reported by Davidse *et al.*[10] except that the slopes are somewhat less than those measured by these authors at 5 kHz. This difference is mainly due to sample shape effects. Since PE is a mixture of crystalline and amorphous domains, the density dependence of the velocity can be expected to reflect the proportion of the crystalline phase present. It can be analysed by the empirical equation for the elastic modulus of a mixed system

$$M^v = \chi M_c^v + (1 - \chi)M_a^v \tag{12}$$

where M and χ denote the modulus and volume fraction of the crystallite. The suffices c and a represent the crystal and amorphous domains. It is usual to place v equal to -1 for a series arrangement and equal to 1 for a parallel arrangement of components.

Since the velocity of the sound wave is given by

$$v = \sqrt{M/\rho} \tag{13}$$

the dependence of the velocity on the fraction of the crystalline phase will be given by

$$\frac{dv}{d\chi} = \frac{A\rho^{-v}}{2} v^{1-2v} - \frac{v}{2\rho}\left(\frac{d\rho}{d\chi}\right) \tag{14}$$

where A is a constant given by

$$A = (M_c^v - M_a^v)/v \tag{15}$$

The velocity, density, crystallinity correlation of *Figure 6* indicates that v has a value of 0.5. The variation of the density with x is approximately $\frac{1}{10}$ of the variation of the velocity of the comparable crystallinity range, justifying the neglect of the second term in equation (15) in the evaluation of the coefficient v. From these data we calculate $dv/d\chi$ as 1.7×10^3 m s^{-1}, compared with the measured value of 1.6×10^3 m s^{-1}.

The physical interpretation lies in the effect of branching, and to illustrate this we present both the velocity and the density as linear functions of the number of branches per 10^3 CH_2 groups (*Figure 12*).

Drawing

The effects of drawing on the velocity of sound have recently been published[2]. However, the effects on the attenuation were not investigated. In this study the density increases with draw ratio while the attenuation decreases (*Figure 13*). (This is in contrast with the behaviour of polypropylene[23]). The attenuation decreases more rapidly than the fraction of the amorphous phase, a result which we interpret as due to a destruction of spherulite morphology[53,54] with reduction in spherulite–phonon scattering.

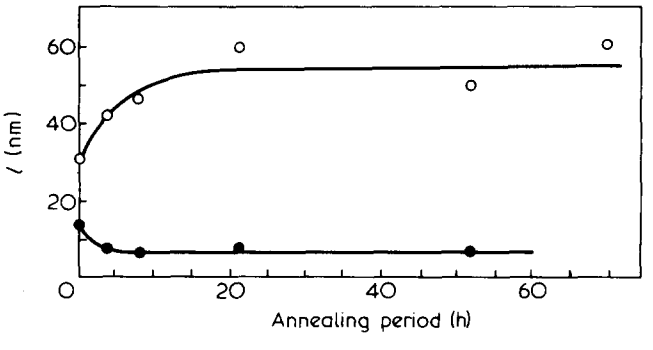

Figure 11 Effect of annealing on the thickness of the crystalline lamellae and amorphous zones. ○, crystalline lamellae; ●, amorphous zones

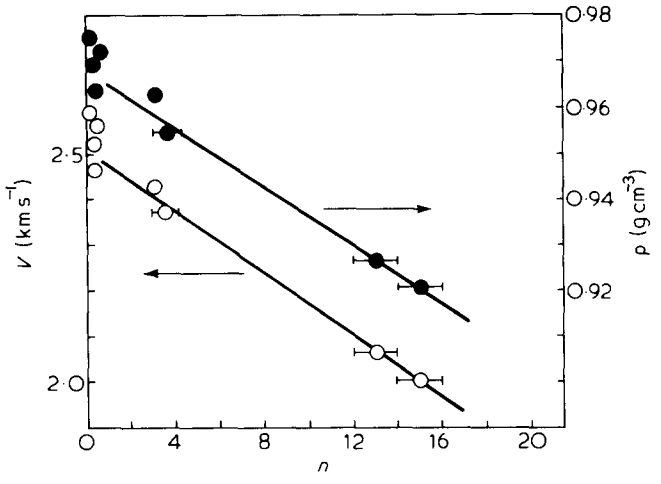

Figure 12 Effect of chain branching on the acoustic velocity and density, *n* denotes the number of branches per 1000 carbon atoms

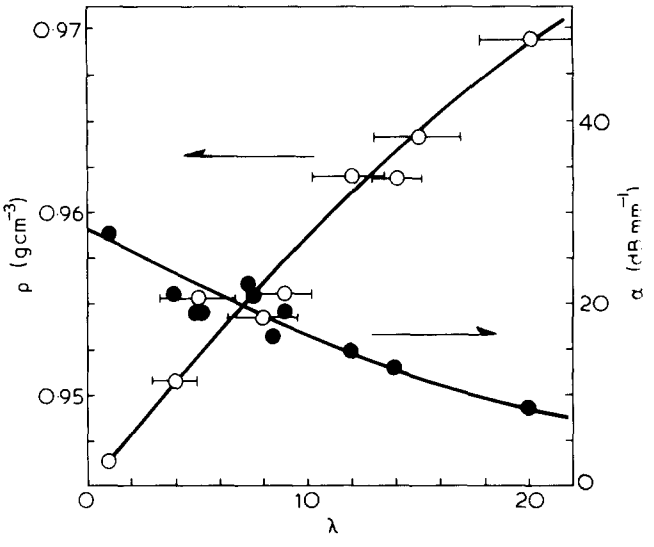

Figure 13 Effect of draw ratio, λ, on the attenuation, α, at 70 MHz (●) and the density (○) for the sample P3 at 298K

Such effects are absent in the low density polymer (P7) as expected.

CONCLUSIONS

Variations in ultrasound velocity and attenuation are attributed to β and γ molecular relaxations, to spherulite–amorphous thermoelastic heat flow and to spherulite–phonon scattering. Chain branching, annealing and drawing all affect the crystallite morphology and thence the acoustic propagation parameters. It is now possible to correlate branching, crystallite morphology, density, ultrasound velocity and attenuation in a self-consistent fashion.

ACKNOWLEDGEMENTS

The authors wish to thank the SRC for the provision of funding to construct the high frequency ultrasonic apparatus and for support for KA during the period of this study through the provision of a research grant. The assistance of Mr T. Wright (University of Glasgow) with assembly and maintenance of the equipment used in these studies is also gratefully acknowledged.

REFERENCES

1 North, A. M., Pethrick, R. A. and Phillips, D. W. *Macromolecules* 1977, **10**, 992
2 Rider, J. G. and Watkinson, K. M. *Polymer* 1978, **19**, 645
3 Perepechko, I. I. and Sorokin, J. E. *Sov. Phys. Acoust.* 1973, **18**, 485
4 Hartmann, B. and Jarzynski, J. *J. Appl. Phys.* 1972, **43**, 4304
5 Folds, D. L. *J. Acoust. Soc. Am.* 1972, **52**, 426
6 Bordelius, N. A. and Semenchenko, J. K. *Sov. Phys. Acoust.* 1971, **16**, 519
7 Asay, J. R. and Guenther, A. H. *J. Appl. Polym. Sci.* 1967, **11**, 1087
8 Arnold, N. D. and Guenther, A. H. *J. Appl. Polym. Sci.* 1966, **10**, 731
9 Eby, R. K. *J. Acoust. Soc. Am.* 1964, **36**, 1485
10 Davidse, P. D., Waterman, H. I. and Westerdijk, J. B. *J. Polym. Sci.* 1962, **59**, 389
11 Schuyer, J. *J. Polym. Sci.* 1959, **36**, 475
12 Baccaredda, M. and Butta, E. *J. Polym. Sci.* 1956, **22**, 217
13 McCrum, N. G., Read, B. E. and Williams, G. 'Acoustic and Dielectric Effects in Polymeric Solids', John Wiley, London, 1967
14 Schmieder, K. and Wolf, K. *Kolloid Z.* 1953, **134**, 149
15 Mansfield, M. and Boyd, R. H. *J. Polym. Sci. Polym. Phys. Edn* 1978, **16**, 1227
16 Iwayanagi, S. *Rep. Prog. Polym. Phys. Jpn.* 1962, **5**, 131
17 Illers, K. H. *Rheol. Acta* 1964, **3**, 211
18 Gray, R. W. and McCrum, N. G. *J. Polym. Sci. Polym. Phys. Edn.* 1969, **7**, 1329
19 Matthew, J., Shen, M. and Schatzki, J. F. *J. Macromol. Sci.* 1977, **B13**, 349
20 Willbourn, A. H. *Trans. Faraday. Soc.* 1958, **54**, 717
21 Roberts, R. M., Gilbert, J. C., Rodewald, L. B., Wingrove, A. S. 'An Introduction to Modern Experiments Organic Chemistry', Halt, Rinehalt and Winston Inc., New York, 1969
22 Randall, J. C. *J. Polym. Sci. Polym. Phys. Edn.* 1973, **11**, 275
23 Datta, P. K. and Pethrick, R. A. *Polymer* 1978, **19**, 145
24 Waterman, H. A. *Kolloid Z.* 1963, **192**, 1
25 Andraeae, J. H., Bass, R., Heasell, E. L. and Lamb, J. *Acustica*, 1958, **8**, 131
26 Wright, T. and Campbell, D. D. *J. Phys. Eng. Sci. Inst.* 1977, **10**, 1241
27 Oakes, W. G. and Robinson, D. W. *J. Polym. Sci.* 1954, **14**, 505
28 Saito, S. and Nakajima, T. *J. Polym. Sci.* 1959, **36**, 533
29 Kline, D. E., Sauer, J. A. and Woodward, A. E. *J. Polym. Sci.* 1956, **22**, 455
30 Takayanagi, M. and Matsuo, T. *J. Macromol. Sci.* 1967, **B1**, 407
31 Tuijnman, C. A. F. *Polymer* 1963, **4**, 259
32 Wada, Y. and Yamamoto, K. *J. Phys. Soc. Jpn.* 1956, **11**, 887
33 Matheson, A. J. 'Molecular Acoustics', John Wiley, London, 1971
34 Bhatia, A. B. 'Ultrasonic Absorption', Oxford Univ. Press, London, 1967
35 Herzfeld, K. F. and Litovitz, T. A. 'Absorption and Dispersion of Ultrasonic Waves', Academic Press, New York, 1959
36 Eiermann, K. *Kolloid Z.* 1965, **201**, 3
37 Brandrup, J. and Immergut, E. H. 'Polymer Handbook Second Edn.', John Wiley, New York, 1975
38 Zener, C. *Proc. Phys. Soc.* 1940, **52**, 152
39 Zener, C. 'Elasticity and Anelasticity of Metals', Chicago Univ. Press, Chicago, 1948
40 Fisher, E. W. *Z. Naturforsch*, 1957, **122**, 753
41 Geil, P. H. 'Polymer Single Crystals', Intersci. Pub., New York, 1963
42 Wunderlich, B. 'Macromolecular Physics', Vol. 1 and 2, Academic Press, New York, 1973
43 Okano, K. 6th Int. Congr. Acoust. (Tokyo) H-61
44 Truell, R., Elbaum, C. and Chick, B. B. 'Ultrasonic Methods in Solid State Physics', Academic Press, New York, 1969
45 Pechhold, W. *Kolloid Z.* 1968, **228**, 1
46 Keith, H. D. and Passaglia, E. *J. Res. Nat. Bur. Stand.* 1964, **68A**, 513
47 Predecki, P. and Statton, W. O. *J. Appl. Phys.* 1966, **37**, 4053
48 Sinott, K. M. *J. Appl. Phys.* 1966, **37**, 3385
49 Woodruff, T. O. and Ehrenreich, H. *Phys. Rev.* 1961, **123**, 1553
50 Kijima, T., Koga, K., Imade, K. and Takayanagi, M. *Polym. J.* 1975, **7**, 14
51 Fischer, E. W. and Schmidt, G. F. *Agnew. Chem.* 1962, **74**, 551
52 Lauritzen, J. I., Jr. and Hoffman, J. D. *J. Res. Nat. Bur. Stand.* 1960, **64A**, 73
53 Hay, I. L. and Keller, A. *Z. Polym.* 1965, **204**, 43
54 Ingram, P., Kiho, H. and Peterlin, A. *J. Polym. Sci. C.* 1967, **16**, 1857